

The effects of dip-limited Kirchhoff migration and F-K migration

Kun Liu and John C. Bancroft

ABSTRACT

Dip-limited migration is utilized in practice for the purpose of either decreasing the computational cost (e.g., Kirchhoff migration) or suppressing noise (e.g., Kirchhoff and F-K migration). Dip-limited F-K migration is a common F-K migration with an embedded dip filter, while the dip-limited Kirchhoff migration is implemented by limiting the aperture of migration operators. Either of these methods will cause a dip-filtering action and result in a dip-restricted output section. However, there are distinctions between the effects of dip-limited Kirchhoff and F-K migration. Dip-limited F-K migration has an exact dip-filtering effect on the migrated section, whereas the dip-limited Kirchhoff migration generates additional artifacts when the dip limit is less than the maximum dip on the desired output section. These artifacts are caused by the endpoints of the migration operators and become more obvious as the dip limit is decreased. A geometric explanation as well as a synthetic experiment is developed in this paper to help understand these effects.

INTRODUCTION

Seismic migration is a wave-equation-based process that removes distortions from reflection records by moving events to their correct spatial locations and by collapsing energy from diffractions back to their scattering points (Gray, 2001). Among the ample variety of migration methods, Kirchhoff migration and F-K migration¹ are used in industrial seismic processing because of their conceptual simplicity and remarkable accuracy-to-cost ratio. In practice, dip limit may be specified in both migration implementations for the purpose of either decreasing the computational cost (for Kirchhoff migration) or reducing noise (for Kirchhoff and F-K migration). The dip-limited Kirchhoff migration can be implemented by limiting the aperture of migration operators, while, in F-K migration, dip-limiting is equivalent to an embedded dip-filtering action.

Similar to the diffraction summation method (Miller et al., 1987), where each image point was considered as a possible diffractor, Kirchhoff migration (2D) first applies a derivative operator and a weighting factor to the unmigrated traces. Then, for each trace, the energy at the time defined by the diffraction traveltime curve is summed and placed at the image point. The range of the summation on the input data is usually limited to a defined spatial interval that, in practice, is called migration aperture. A good-quality migrated image requires a migration aperture with optimal size. An excessively small aperture causes suppression of steeply dipping events, while an excessively large aperture means significant time cost without quality improvement (Schleicher et al., 1997; Sun, 1998). More importantly, large apertures will degrade the migration quality in poor signal-to-noise ratio conditions (Yilmaz, 1987; Bancroft 1998).

¹ There are two major types of migration based on Fourier transforms: Stolt's constant velocity migration and Gazdag's phase-shift migration (other migrations may also use the Fourier transform as part of their algorithms). Only Stolt F-K migration is discussed in this paper.

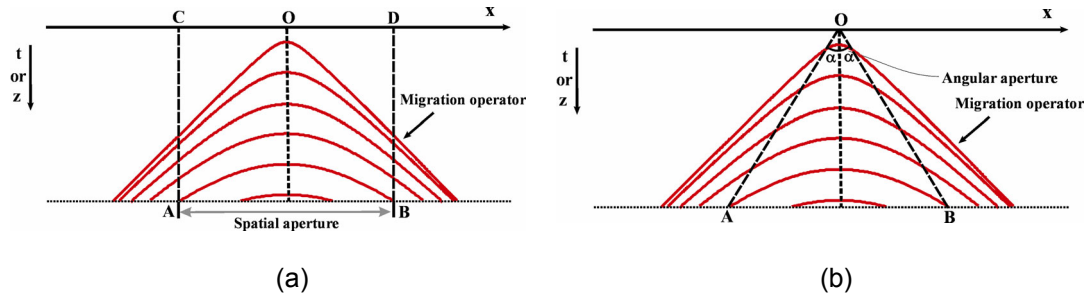


FIG. 1. The spatial aperture (a) and angular aperture (b) in Kirchhoff migration.

The spatial aperture or extent that the actual summation path spans can be defined as the number of traces (Yilmaz, 1987) and identified in Figure 1(a) by the vertical lines CA and DB. Alternatively, an “angular aperture”, defined by the angle AOB (2α) in Figure 1(b), was also suggested (e.g., Promax manual). For the given diffraction in Figure 1(b), the spatial extent of the summation path is equal to the range confined by the angular aperture at points A and B, and thus, it varies with the depth of the image point. Defining aperture in terms of angle is similar to imposing a dip limit on the migration operators and consequently limiting the dip range on the migrated section. In regions where dips are known to be restricted, this is a very convenient way of reducing operator aliasing and improving computational efficiency at the same time (Hertweck, 2002). Further, this implementation can attenuate the noise at shallow times by using the smaller operators (Bancroft, 1998). Therefore, in this paper, the angular aperture, instead of the fixed-width one, will be used in the following discussions. In addition, due to the symmetry of migration operators, half angular aperture α will be referred as the “aperture”.

It should be pointed out that both of the aperture definitions could lead to the dip-limited migration operators. In the case of constant velocity, the specification of a fixed-width “spatial aperture” will result in the migration operators (hyperbolas) with various maximum dips at their endpoints (Figure 1(a)). Under the definition of “angular aperture”, however, the migration operators will have an identical maximum dip angle (Figure 1(b)), which is similar to the dip-limited F-K migration and also to the dip-limited finite difference migration algorithms. The situation becomes more complicated if the medium velocity varies, but that won’t be covered in this paper. The main purpose of this paper is to evaluate the artifacts from a dip-limited Kirchhoff migration when compared to those from a dip-limited F-K migration.

In general, dip-limited migration causes a dip-filtering effect upon the migrated section. Dip-limited F-K migration has an exact dip-filtering effect and can remove all the energy above a defined dip limit. Note that, in practical application of F-K migration, there are considerations to minimize other features, e.g., zero padding and complex interpolation utilized to avoid wrapping around. These considerations have been included in the migration algorithm but attention will be mainly focused on the dip-limiting effects, assuming other artifacts are successfully suppressed.

In dip-limited Kirchhoff migration, however, cautions should be taken to ensure the assigned dip limit exceeds the maximum dip of the migrated section. Otherwise, the energy from the dipping events, excluded by the dip limit, may become the shallower artifacts on the migrated section. As shown later, these artifacts are caused by the endpoints of the migration operators.

A constant-velocity earth model consisting of various dipping reflectors is first built, and then, the synthetic section is generated and used as the input data to show the various effects of dip-limited Kirchhoff time migration and F-K migration. Meanwhile, a geometrical explanation on the artifacts from dip-limited Kirchhoff migration is also presented.

DIP-LIMITED KIRCHHOFF MIGRATION

When investigating the dip angles in a seismic section, it is important to distinguish them on the time and depth sections. With the assumption of constant velocity, we will start the discussion first in the depth domain by plotting the travel distance vertically to simulate the seismic recording. It's valid since depth to time conversion can be done simply by a 1-D stretching.

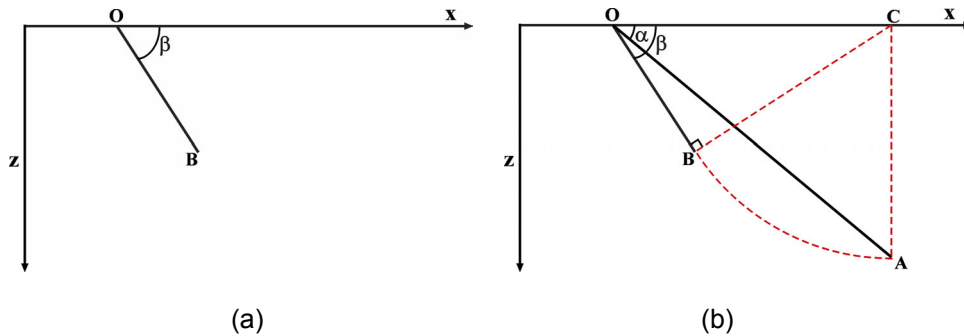


FIG. 2. (a) A dipping reflector with the dip angle of β . (b) Map the travel distance BC in the z direction to obtain the recorded event OA with the dip angle of α .

Consider a simple constant-velocity earth model containing a dipping reflector OB with the dip angle of β in Figure 2(a). The source and receiver are both located at C (Figure 2b). The ray from C will be reflected at B and recorded at C. The travel distance BC is mapped vertically on the x-z plane as in Figure 2(b) to the segment AC with the dip angle of α . The event OA could be plotted with a vertical scale into the time section and Figure 2(b) may be regarded as its apparent depth section. It's easy to derive the following relationship,

$$\tan(\alpha) = \sin(\beta), \tag{1}$$

which is known as the “migrator’s equation” (Robinson, 1983, 456) that describes the relationship between the migrated dip β and recorded dip α .

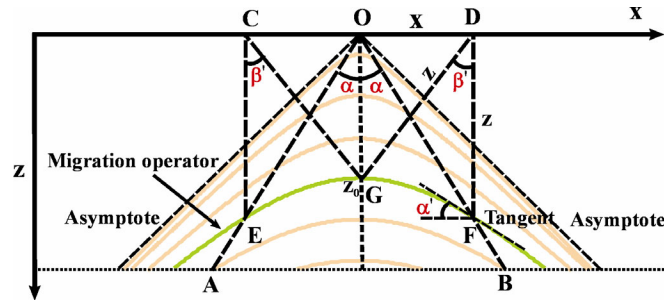


FIG. 3. Angle relationship with the migration operator.

Similarly, the dip-limited Kirchhoff migration may also be illustrated in the depth section when the velocity is constant. Figure 3 contains a scatter point G located at the depth of z_0 . A source-receiver pair is moving across the surface with a displacement x from the surface location of the scatter point. A record section on the depth plane is generated by mapping the travel distance in the z -direction as shown in Figure 3. The relationship between the displacement (x) and the travel distance (z) from the scatter point to each source-receiver pair is derived as,

$$z^2 - x^2 = z_0^2, \quad (2)$$

which is a hyperbolic equation. The shape of the hyperbola is governed by the location of its apex (z_0). By varying z_0 , a family of hyperbolas is drawn, according to the equation (2), with their apexes at the same x coordinates in Figure 3. Those hyperbolas can be regarded as the migration operators when Kirchhoff migration is implemented in the x - z domain. If the migration aperture (angle GOB or GOA) is chosen as α that is equal to the angle AOC in Figure 2(b), and angle GDF or GCE is defined as β' , the following relationship can be immediately derived from Figure 3 as,

$$x = z \tan(\alpha) = z \sin(\beta'), \quad (3)$$

or

$$\tan(\alpha) = \sin(\beta'). \quad (4)$$

Comparing equation (4) and equation (1), it is obvious that $\beta' = \beta$, i.e. if the angular migration aperture is chosen as the unmigrated dip angle α , the angle GDF or GCE is then equal to the desired migrated dip angle β . Here, only the segments of operators confined by AOB are involved in the migration.

The specification of the angle α for the migration aperture will limit the dip on the migration operator and consequently limit the dip on the migrated section. By differentiating equation (2), the slope of the tangent at F (Figure 3) on a single operator is calculated as,

$$\tan(\alpha') = \left(\frac{dz}{dx}\right)_F = \frac{x_F}{z_F} = \tan(\alpha), \quad (5)$$

or

$$\alpha' = \alpha \quad (6)$$

Therefore, when the migration aperture is given as α , the maximum dip on the migration operator is α , too. According to equation (4), the dip on the migrated section will be limited to β . A geometric demonstration of dip-limited Kirchhoff migration is shown below where angle GDF (or GCE) in Figure 3 is referred as the “dip limit” parameter.

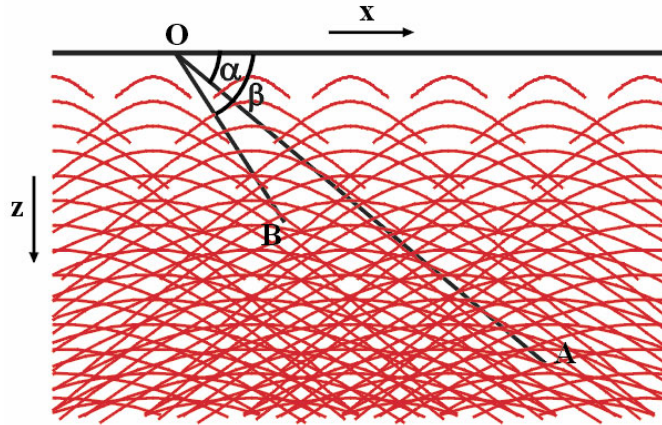


FIG. 4. Zero-offset section with a single dipping event OA at the dip of α (40°). After migration, OA should be migrated to OB with the dip of β (57°). When the dip limit (angle GCE or GDF in Figure 3) is equal to β (57°), the migration operators are limited by α (40° , from equation (4)) and indicated by the truncated hyperbolas superimposed on the input section.

The section containing a single dipping event OA with the dip angle of α (40°) is used as input data to illustrate the effects of dip-limited Kirchhoff migration (Figure 4). The dip limit parameter (defined as angle GDF or GCE in Figure 3) is set to β (57°), i.e., the expected dip angle after migration. Given the previous discussion, the migration aperture can be deduced from equation (4) as α (40°). Figure 4 illustrates the input section superimposed by the desired reflector OB and migration operators limited by α (40°). Note that the shape of hyperbolas is the same when their apexes are at the same depth due to equation (2). Only the operators whose apexes lie on OB are plotted in Figure 5(a). Based on the Kirchhoff migration theory that energy summation is implemented along the operator into its apex, those operators are the only ones contributing to the final image of OB. Since the aperture of migration operators is limited to α (40°), angles $A_1O_1A_1'$, $A_2O_2A_2'$, $A_3O_3A_3'$ and $A_4O_4A_4'$ are all equal to α (40°). Keep in mind that α is also the dip of OA, from equation (6) we can conclude that the right end of each operator must be tangential to OA. During migration, energy at the tangential points is gathered, summed and weighted properly along the operators into their apexes where the migrated image, OB, is formed. Note that, for true-amplitude reconstruction, the migration aperture should be confined by the points, where the difference between the travel-times of reflected (e.g., OA in Figure 5(a)) and point-diffracted rays (e.g., migration operators in Figure 5(a)) equals the duration of the recorded seismic pulse (Schleicher, 1997; Sun, 1998). That is, to guarantee the true amplitude of OB, the optimal migration aperture should be bigger than the one shown in Figure 5(a). Here, figure 5(a) should be understood in a qualitative sense.

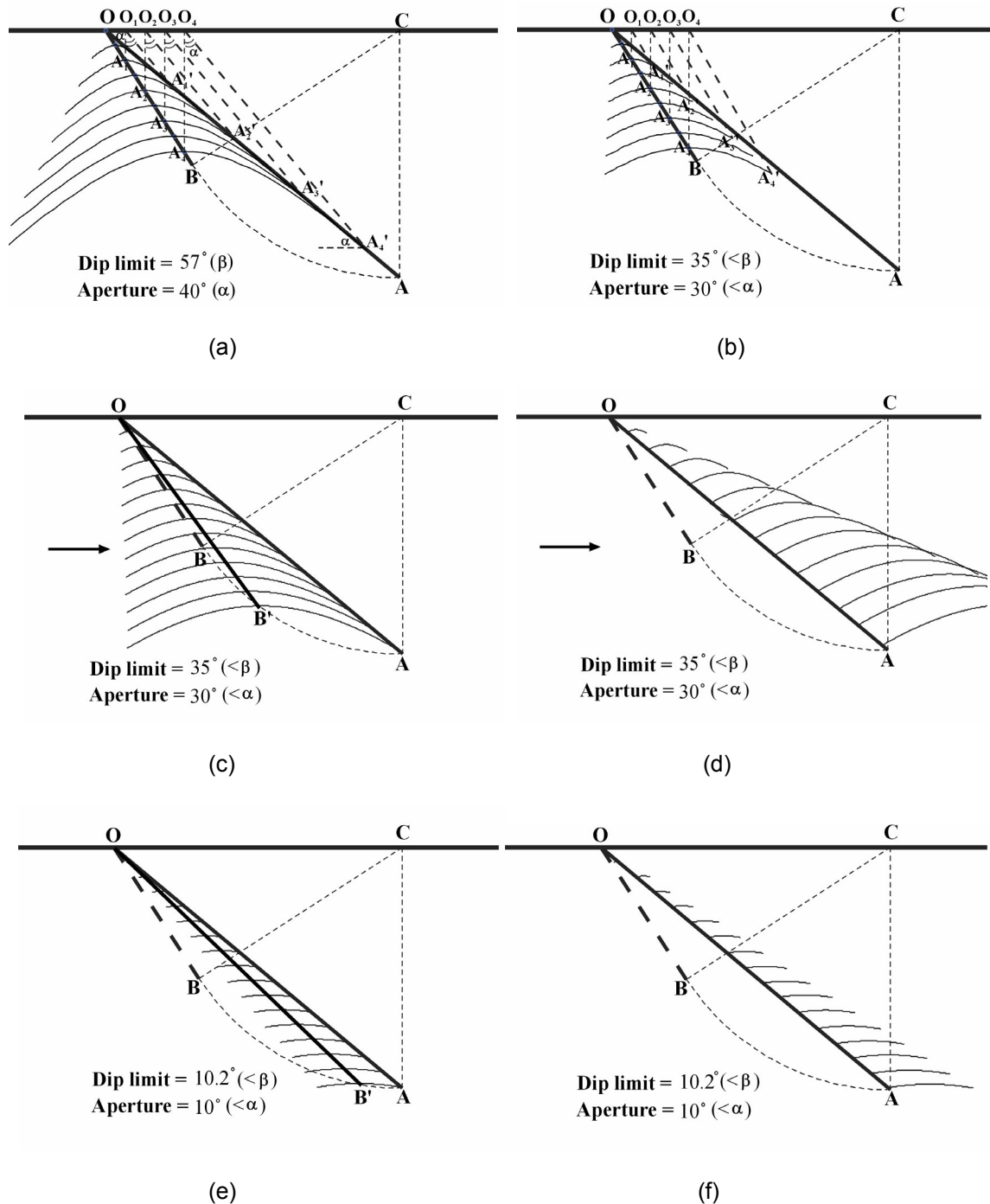


FIG. 5. The effects of dip-limited Kirchhoff migration. (a) The dip limit is equal to β (57°); (b) The dip limit is less than β (35°). This results in a dip-filtering effect on the migrated section; (c) When the right endpoints of the operators intersect with OA, there may still exist a residual event OB' whose dip is less than the desired dip after migration; (d) Migration noise may also occur when the left endpoints of the operators intersect with OA; (e) The extreme case when the aperture is very small. Little migration effects are presented. (f) Same effects as shown in (d) but with shorter aperture.

What happens if the dip limit parameter is chosen less than the desired dip β (57°)? For example, when dip limit is equal to 35° (Figure 5(b)), from equation (4), the migration aperture changes into 30° (less than α (40°)), and the right endpoints of the operators, i.e. A_1' , A_2' , A_3' and A_4' , are no longer on OA. Thus, no energy will be summed into their apexes resulting in the absence of OB. However, there may exist a “migrated” image of OA. For the operators whose right endpoints intersect with OA (Figure 5(c)), energy will be gathered and summed into the apex at an incorrect position (OB' in Figure 5(c)) where the migrated dip is smaller than the desired dip β . In consequence, dip-limited Kirchhoff migration causes a dip-filtering effect on the migrated section, but generates artifacts when the dip limit parameter is chosen less than the maximum desired dip on the migrated section. For the extreme case when dip limit is very small (10.2° in Figure 5(e)), the migrated event is very close to OA, indicating that the event in the input section is almost unmigrated.

The other two possibilities are (1) migration operators cross over OA and (2) the left endpoints of operators intersect with OA (Figure 5(d) and (f)). For the former case, the energy gathered from the cross section will tend to cancel out (assume no operator aliasing), while, for the latter case, migration noise may occur again due to the incomplete destruction.

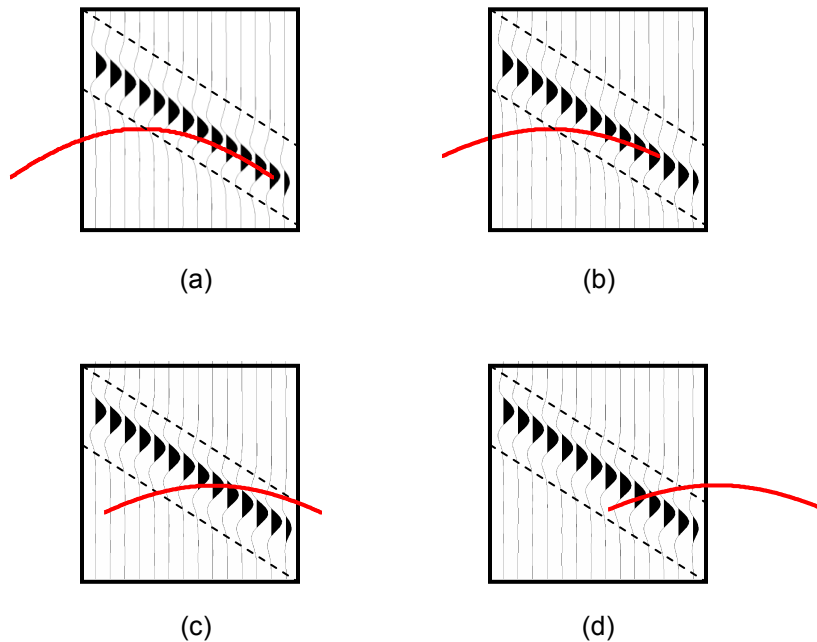


FIG. 6. Schematic interpretation on migration effects. The two dash lines confine the main energy of the dipping event. (a) Migration aperture is equal to the dip of the event. Migration signal can be formed when the operator is tangential to the event; (b) Migration aperture is less than the dip of the event and generates artifacts from the right endpoint; (c) No artifact will occur when operator crosses over the event (assume no operator aliasing); (d) Artifacts may be caused from the left endpoint of the operator.

Figure 6 gives a schematic interpretation on the effects in Figure 5. Assume in Figure 6 that the main energy of the dipping event lies in the area confined by the two dash lines. When the migration aperture is equal to the dip of the event (Figure 6(a)), the operator can be tangential to the dipping event and energy will be summed along the operator to

give the migration signal. Whereas, when the aperture is less than the dip of the event (Figure 6(b)), the migration operator couldn't be tangential to the event and artifacts may occur. As long as the right endpoint of the operator lies in the dipping energy area, migration noise could occur until the operator crosses over the event (Figure 6(c)). After that, energy picked up by the migration operator tends to cancel out. It's also possible that the left endpoint of the migration operator falls in the dipping energy area and causes artifacts (Figure 6(d)). These are not the typical artifacts from the dip-limited Kirchhoff migration because the left endpoint will intersect with the event no matter what the dip limit is chosen as. The degree to how serious the migration noise is depends on the specified dip limit, taper size and the dip of the event. Sun (1998) provided a theoretical explanation on the artifacts caused by the endpoints of migration operators by using the method of stationary phase in high-frequency approximation (Bleistein, 1984, 77-82). Qualitatively, for the example shown in Figure 6 where the dipping event extends downward to the right, the artifacts caused by the right endpoint may be the dominant artifacts because the contribution from the right endpoint is more than that from the left endpoint. However, it's only a rough estimation and strict validation should be referred to the work by Sun (1998).

For Kirchhoff time migration, the input and output sections are both in x-T domain. If the velocity of the medium V is constant, equation (2) can be converted to,

$$T^2(x) = T_0^2 + \frac{4x^2}{V^2}, \quad (7)$$

where T_0 is the two-way vertical traveltime from z_0 to the surface. The curve defined by equation (7) is the migration operator (hyperbola) in the time domain. Based on the former discussions in the depth domain, dip-limited Kirchhoff time migration may be implemented in a similar way.

Note that, in the time domain, both unmigrated and migrated dip angles depend on the velocity V (see, e.g., Chun and Jacewitz, 1981). In order to utilize the angle relationships deduced previously in the depth section, we first convert the input time section into the apparent-depth section. In the case of constant velocity, the migration operators can be converted from unmigrated time section to unmigrated depth (apparent depth) section by simple 1-D stretching. Thus, the maximum half width x_{\max} of the migration operator can be computed from Figure 3 by,

$$x_{\max} = \frac{T_0 V \tan \bar{\beta}}{2}, \quad (8)$$

where $\bar{\beta}$ is the dip limit parameter related to the angular aperture by equation (4). Since there is only vertical stretch in the time and depth conversion, the calculated extent of migration operators ($2x_{\max}$) in unmigrated depth section can be used back in unmigrated time section. Consequently, Kirchhoff migration can be implemented in the time domain along these limited migration operators with a spatial extent varying with time (T_0), which results in a dip-limited output section. For the same reason discussed before,

artifacts can be observed from the output time section when dip limit parameter $\bar{\beta}$ is set less than the maximum dip in the desired migrated section.

DIP-LIMITED F-K MIGRATION

Stolt (1978) established a frequency domain migration by utilizing the 2-D Fourier transform for the post-stack zero-offset case. The algorithm, limited to constant velocity, is simple and efficient, and was a major workhorse in industrial processing in 1980's. The Stolt F-K migration begins by Fourier transforming the input traces from time and space coordinates (x, t) into frequency-wavenumber (k_x, ω) domain, then moves the amplitude and phase at each (k_x, ω) to their corresponding (k_x, k_z) location. A complex-valued interpolation will be required during the mapping process. The desired image is eventually obtained by inverse Fourier transforming the resulted (k_x, k_z) coordinates back to (x, z) domain. Detailed introduction for the Stolt F-K migration can be found in former publications (e.g., Stolt, 1978; Chun and Jacewitz, 1981; Yilmaz, 1987, 263), and thus won't be covered in this paper.

Dip-limited F-K migration is actually the F-K migration plus a dip-filtering action while the data are in the (f, k) domain. One may consider them as two separate steps, but here, in order to compare the effects between Kirchhoff and F-K migration, we combine them into one algorithm and name it as the dip-limited F-K migration. Theoretically, the dip-limited F-K migration will give exact dip-filtering effects on the migrated section because a rejection fan (2-D filter) can be directly imposed upon the F-K domain to exclude the unwanted dips. In practice, a filter with sharp boundaries will result in Gibbs oscillations that appear in the filtered section. These artifacts, though, can be greatly attenuated by tapering the filter boundaries. In addition, given a dip limit, the dip filter tends to exclude the higher dip energy as well as keep the lower one. This lower dip energy may contribute to the event that is desired to be removed on the output section and hereby causes the artifacts (see synthetic example below).

Dip-limited F-K migration causes exact dip-filtering effects on the migrated section, while the dip-limited Kirchhoff migration generates artifacts when the dip limit is chosen less than the desired dip on the migrated section. The distinctions become more obvious when decreasing the dip limit of the migration. A synthetic example will be shown below to illustrate this point.

SYNTHETIC EXAMPLES AND DISCUSSION

A simple earth model (Figure 7) was built to test and compare the effects of dip-limited Kirchhoff and F-K migration. Four dipping reflectors in the model have dip angles of 0° , 30° , 45° and 60° , respectively. A constant velocity of 2Km/s is assumed for the model, and it is assumed that reflections will occur because of density contrasts. If the source and receiver are placed at the same location along the surface, the recorded (synthetic) section will be a diffracted seismogram of Figure 8. This synthetic zero-offset section is generated by utilizing the modeling function "*susynlv*" in Seismic Unix (Cohen and Stockwell, 2001), which is a Kirchhoff-type modelling program. The unit of horizontal axis (distance) is in kilometre with the trace interval of 10m, and the unit of vertical axis (two-way travelttime) is second at the sampling rate of 0.002s. A taper of 10°

is applied to both the migration operators in Kirchhoff migration (Sun, 1998; Hertweck, 2002) and the dip filters in F-K migration to minimize the migration noise caused by abrupt truncation.

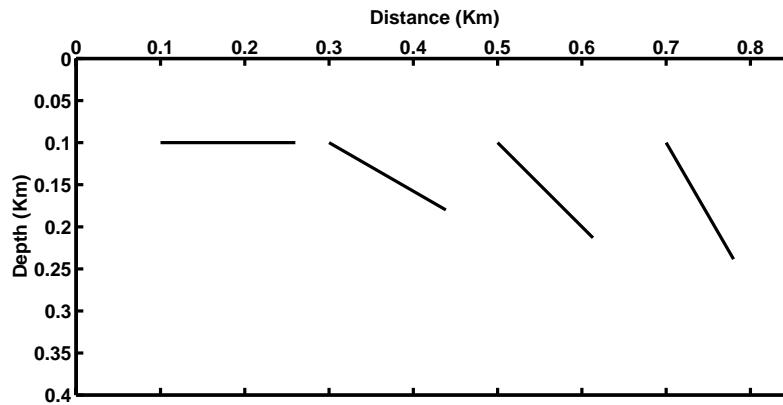


FIG. 7. The earth model containing four dipping reflectors with the dip angle of 0°, 30°, 45° and 60°, respectively.

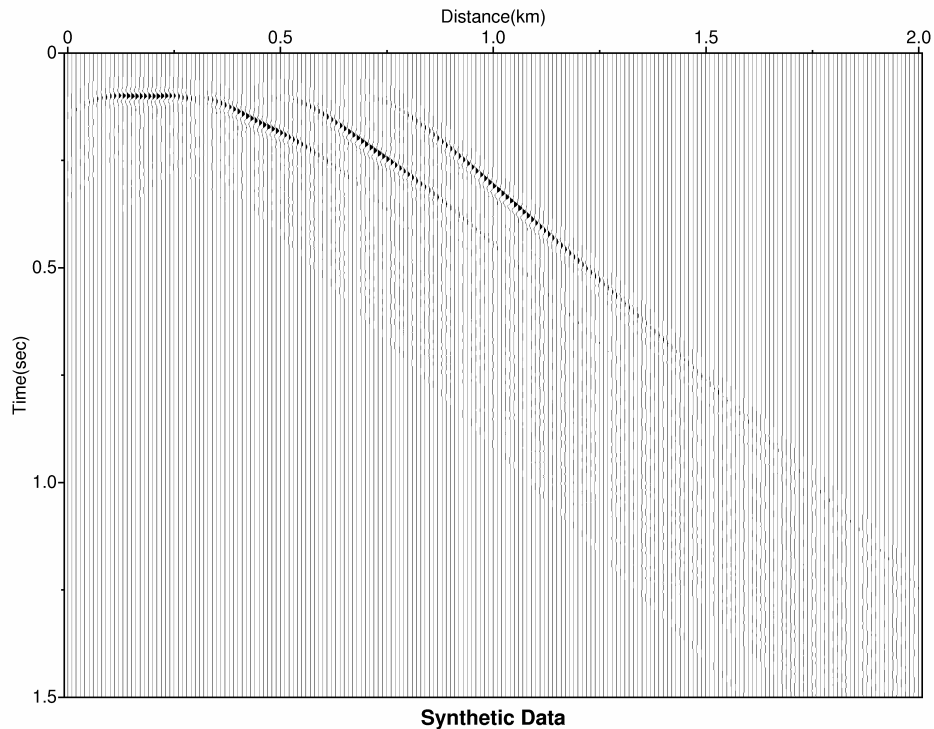


FIG. 8. The zero-offset synthetic data for earth model in Figure 7.

The migrated sections without dip limit² are shown in Figure 9(a) (Kirchhoff migration) and Figure 9(b) (F-K migration). The solid lines in Figure 9 denote the true subsurface positions of reflectors in the earth model. By choosing the constant velocity of 2Km/s, the time and depth coordinates become interchangeable, thus the reflectors in the

² Actually, for Kirchhoff migration, the aperture is always dip-limited. Here we used a very big aperture to approximate the ideal result.

model can be directly superimposed on the migrated time sections for convenient comparison. In the absence of dip limit, i.e., full aperture width in Kirchhoff migration and no dip filtering in F-K migration, the migrated sections are perfectly coherent with the earth model as indicated by Figure 9.

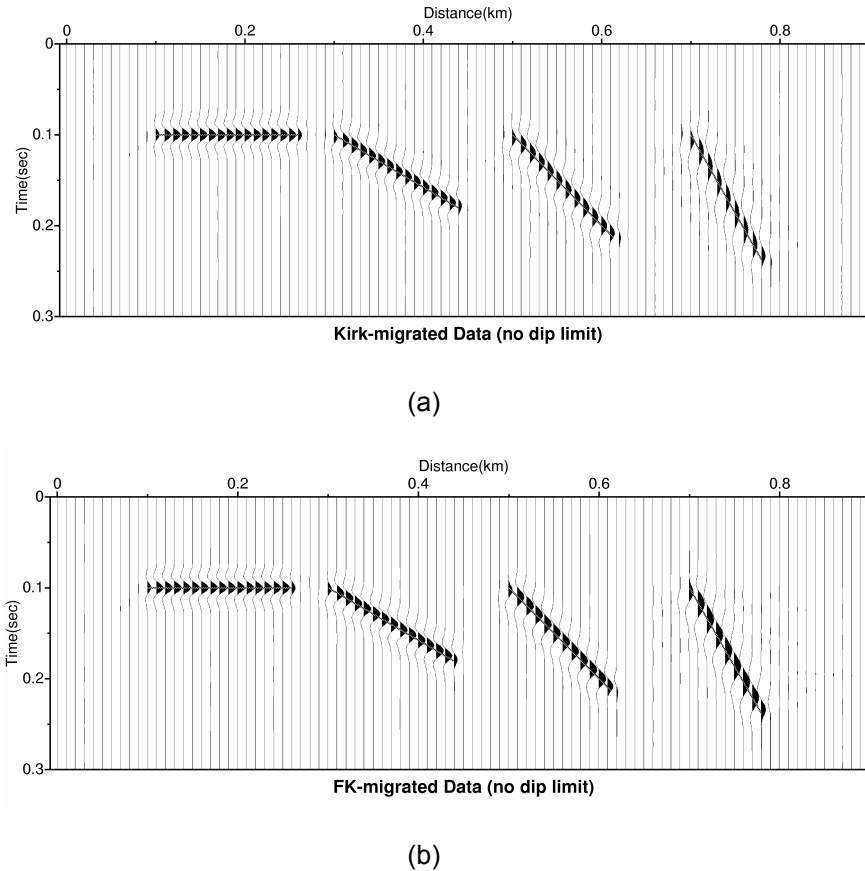


FIG. 9. The migrated sections using Kirchhoff migration (a) and F-K migration (b) with no dip limit.

The effects of dip-limited Kirchhoff and F-K migration are now considered shown by Figure 10. The migrated sections without dip limit (Figure 9(a) and (b)) are re-plotted as Figure 10(a) and (b) for comparison. In both migrations, dip limits are set as 55° , 40° , 25° , 10° and 1° , corresponding to the migrated sections of Figure 10(c) and (d), (e) and (f), (g) and (h), (i) and (j), (k) and (l), respectively. Again, provided the interchangeability of time and depth axis, the desired reflectors are superimposed on the migrated time sections for convenient discussion.

As illustrated in Figure 10(c) and (d), the 60° dipping events (the rightmost events) are filtered out from both migrated sections when dip limit of 55° is specified. Meanwhile, other events with dip angles less than 55° are preserved after the dip-limited migrations. However, when looking into Figure 10(c), the Kirchhoff migrated section, there still exists residual dipping energy in the filtered area with the dip less than 60° . As we discussed in the previous section, the artifacts are actually caused by the right endpoints of the migration operators when aperture is less than the dip of the event. We can also observe some subtle noise in Figure 10(c) when the dips of the events are lower (e.g., the

ringing above the first and second events). It is partly caused by the left endpoints of the operators (also has the contribution of the right endpoints). Note that the artifacts are attenuated with the taper applied to the migration operators.

For the F-K migrated section (Figure 10(d)), the 60° dipping event is completely removed except some subtle noise around the end points of the reflectors. This is because the higher dip energy, which would be required to construct the end points of the reflectors, has been filtered out. Meanwhile, the lower dip energy of the end points remains in the pass band of the dip filter and occurs on the output sections without being canceled out. It's apparent when looking through all the F-K migrated results, where the dips of the noise decrease with the dip limit of the filters.

When the dip limit is decreased into 40°, similar changes happen to the third events in Figure 10(e) and (f) whose dip angles should have been 45° after migration. Note that the dip angle of the fourth event in Figure 10 (e) is less than that in Figure 10(c). The effects become more obvious in Figure 10(g) to Figure 10(j), where dip limits are 25° and 10°, respectively. As compared to the F-K migrated sections (Figure 10(h) and (j)) showing the exact dip filtering effects, the Kirchhoff migrated sections (Figure 10(g) and (i)) contain the artifacts “floating” above the desired reflectors. Even the horizontal events become diffracted in Figure 10(g) and (i), whereas they are little changed in the F-K migrated sections. The artifacts contributed by the left endpoints become more serious as well. It may be explained qualitatively by the fact that the contribution from left endpoints becomes bigger when the aperture decreases.

The extreme examples are shown in Figure 10(k) and (l) where the dip limit is nearly zero (1°). As a result, the aperture of Kirchhoff migration that was related by the dip limit is too small to be able to generate the perceivable migration effects in Figure 10(k), and each event remains unmigrated that is identical to the input section. But no significant change can be observed from the F-K migrated section (Figure 10(l)).

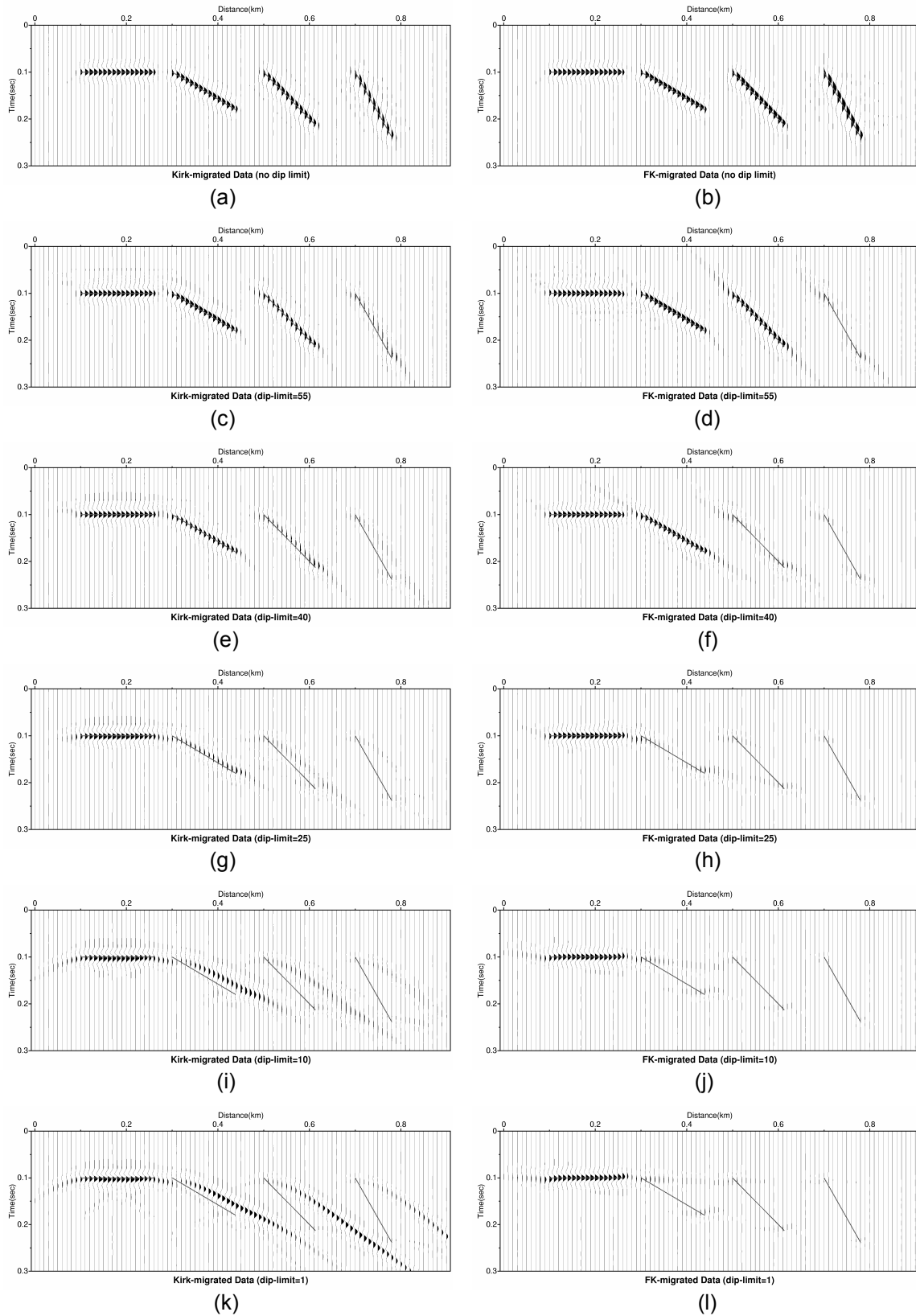


FIG. 10. The effects of dip-limited Kirchhoff migration (left column) and F-K migration (right column).

CONCLUSIONS

Kirchhoff and F-K migration algorithms can be dip-limited. The advantages of the dip-limited migration include decreasing the computational expense (e.g., in Kirchhoff migration) as well as suppressing noise (e.g., in Kirchhoff and F-K migration). When dealing with a large data set, it becomes important for Kirchhoff migration to limit its summation aperture by using a dip limit instead of the default maximum summation width, such that, economical time cost can be acquired and a more even saving is achieved.

The implementation of dip-limited Kirchhoff migration and F-K migration will both cause dip-filtering actions upon the migrated section. However, they demonstrate different effects even though they are both called “dip-limited migration”. The dip-limited F-K migration is actually the common F-K migration embedded with a dip filter. Except for the noise shown before, the dip-limited F-K migration has an exact dip filtering effect on the migrated section, i.e., the dipping events whose dip angles are bigger than the dip limit will be removed from the migrated section.

For the dip-limited Kirchhoff migration, the dip limit is directly related to its summation aperture. Specifying a dip limit will confine the dip on the migration operators and hereby limit the dip on the migrated section. By migrating the synthetic data and comparing the results, it turns out, unlike dip-limited F-K migration, dip-limited Kirchhoff migration generates shallower artifacts when dip limit is chosen less than the desired dip on the migrated section. The artifacts are actually generated from the endpoints of the migration operators and become more obvious as the dip limit being decreased. For the extreme case, i.e., the dip limit is approximately zero, the input section remains unmigrated after Kirchhoff migration, other than the expected effects illustrated by the F-K migrated output. Geophysicists must be cautious, when designing the dip limit parameter in Kirchhoff migration, to ensure the dip limit exceeds the maximum desired dip on the migrated section.

The application of the taper to the operators in Kirchhoff migration is effective in attenuating the artifacts as shown by previous examples. Sun (1998) discussed the taper size in a theoretical manner, but the optimal taper size in practice is still worthwhile to be investigated.

ACKNOWLEDGEMENTS

The authors wish to thank Dr. Gary Margrave and Dr. Larry Lines for their beneficial comments on this research when it was first presented as a course project. We also would like to thank Dr. Hugh Geiger and Thomas Hertweck (Wave Inversion Technology (WIT), Karlsruhe University) for the helpful suggestions and Mark Kirtland for reading and correction of the manuscript.

REFERENCES

- Bancroft, J.C., 1998, Dip limits on pre- and poststack Kirchhoff migrations, CREWES Research Report, **10**, 25.
Bleistein, N., 1984, Mathematics of wave phenomena: Academic Press, Orlando.

- Chun, J.H. and Jacewitz, C.A., 1981, Fundamentals of frequency domain migration: *Geophysics*, **46**, 717-733.
- Cohen, J.K. and Stockwell, Jr. J.W., 2001, CWP/SU: Seismic Unix Release 35: a free package for seismic research and processing, Center for Wave Phenomena, Colorado School of Mines.
- Gray, S.H., 2001, Seismic migration problems and solutions: *Geophysics*, **66**, 1622-1640.
- Hertweck, T., Jäger, C., and Goertz, A., 2002, On the aperture effects in 2.5-D Kirchhoff migration: 72nd Ann. Internat. Mtg., Soc. Expl. Geophys., Expanded Abstracts, 1121-1124.
- Miller, D., Oristaglio, M., and Beylkin, G., 1987, A new slant on seismic imaging: Migration and integral geometry: *Geophysics*, **52**, 943-964.
- Robinson, E.A., 1983, Migration of geophysical data: International Human Resources Development Corp, Boston.
- Schleicher, J., Hubral, P., Tygel, M., and Jaya M.S., 1997, Minimum apertures and fresnel zones in migration and demigration: *Geophysics*, **62**, 183-194.
- Stolt, R.H., 1978, Migration by Fourier transform: *Geophysics*, **43**, 23-48.
- Sun, J., 1998, On the limited aperture migration in two dimensions: *Geophysics*, **63**, 984-994.
- Yilmaz, O., 1987, *Seismic Data Processing*: Soc. Of Expl. Geophys, Tulsa.